THE MARS GLOBAL DIGITAL DUNE DATABASE (MGD[3]): COMPOSITION AND STABILITY. L. K. Fenton[1], A. L. Gullikson[2], R. K. Hayward[2], H. Charles[3], T. N. Titus[2], [1]SETI Institute (189 S. Bernardo Ave., Suite 100, Mountain View, CA 94043, lfenton@seti.org), [2] U.S. Geological Survey (Astrogeology Science Center, 2255 N. Gemini Drive, Flagstaff, AZ, 86001), [3] University of Arizona, AZ.

Introduction: Windblown sand dunes are one of many distinct aeolian features that have shaped the martian landscape. Many important questions about the large dark dunes remain unanswered, such as: To what extent does aeolian sand composition represent the surrounding surface? What is the provenance of dune sand and how did it form into wind-mobilized grains? How have aeolian sands been altered from their source materials? A global look at dune field activity and bulk composition provides a framework from which these questions may be addressed.

The Mars Global Digital Dune Database (MGD[3]) archives the location and several morphological characteristics of dark dunes on Mars [1-3]. The expansion introduced here includes compositional, morphological, and thermophysical characteristics for select dune fields in the MGD[3]. As with the previous installments of the MGD[3], this update has been archived as a U.S. Geological Survey Open-File Report (OFR) by Gullikson et al. (2018), and can be accessed at https://doi.org/10.3133/ofr20181164. Here we address initial results of the compositional and morphological analysis (thermal properties are discussed by [4,5]).

Methods: *Compositional analysis*. We extracted TES data using JMARS [6] and processed with DaVinci [7] dune fields >300 km^2 between 90ºS-65ºN with ocks ("orbit counter keeper") <7000. After removing atmospheric endmembers [e.g., 8], we used a non-negative least squares fitting routine to unmix spectra [e.g., 9] using the spectral library of [10,11]. This resulted in an endmember mineral assemblage comprising 44 minerals that were then binned into eight mineral groups. A mineral confidence index (MCI) with a value of 1 through 3 was calculated for each dune field, based on the number of spectra used and the magnitude of the resulting root-mean-square error (RMSE), as a simple metric of the robustness of the resulting mineral abundances. Of the 79 dune fields spectrally unmixed, 62 produced relatively robust results (MCI = 1 or 2).

Morphological stability. We cataloged the presence or absence of features interpreted to indicate a lack of aeolian activity (i.e., stabilization), using the classification of [12] and extending it to include all MGD[3] dune fields from 90ºS to 75ºN. Dune fields with no apparent stabilization features were assigned a Stability Index (SI) of 1. SI values from 2 through 6 were assigned to dune fields with increasing prevalence and magnitude of stabilization features (e.g., rounded dune brinks, presence of a sharp-edged sand apron around the dune field, a dissected surface, ease of dune type identification). An additional SI confidence index was assigned to each classification, in which values of 1 through 3 indicated good through poor confidence in SI classification (e.g., poor image quality could lead to a confidence index of 2 or 3).

Table 1. Dune field bulk mineral group abundances

Mineral Group	Mean (wt'd) Abundance	Range (MCI = 1 & 2)
Feldspar	28%	13-40%
High-Silica Phases	25%	13-38%
Pyroxene	25%	15-37%
Sulfate	8%	4-17%
Olivine	6%	0-16%
Carbonate	5%	1-7%
Hematite	2%	0-8%
Quartz	1%	0-8%

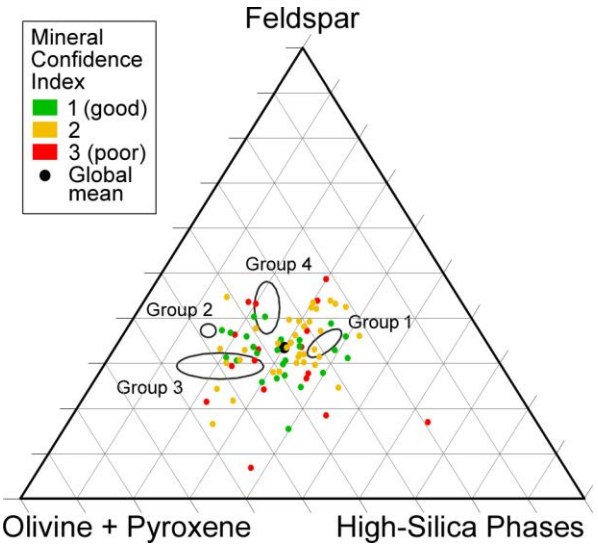

Figure 1. Ternary diagram of the major mineral groups. Modal mineralogic groups from [13] are shown in comparison. Ternary plot from [14].

Results: *Global dune field composition.* **Table 1** lists the weighted mean of the bulk mineral group abundances for the 62 dune fields with MCI values of 1 or 2. Similar to other studies [e.g., 15], TES data indicated that the dunes are predominantly made of feldspar (mainly plagioclase), high-silica phases, and

pyroxene. Twelve dune fields have Sulfate group abundances >~10%, suggesting that sulfates may be present as a minor component of some dune fields. Olivine is thought to be detectable at abundances >~5% [e.g., 16], which is exceeded in 36 of the dune fields, making olivine a common minor component.

Figure 1 compares dune field mineral group abundances with four endmember groups found by [17] to encapsulate the compositional range of low albedo surfaces on Mars. Most dune fields in our study fell within or between these endmembers. Mixtures of Groups 1, 3, and 4 predominate in the mid- to high-southern latitudes [17], where most of the dune fields are located. Thus, to first order, dune sand is representative of the surrounding terrain.

Figure 2 shows the global distribution of the dune fields. Most are located south of 40ºS: only 7 are located north of 40ºS, and none are north of 27ºN.

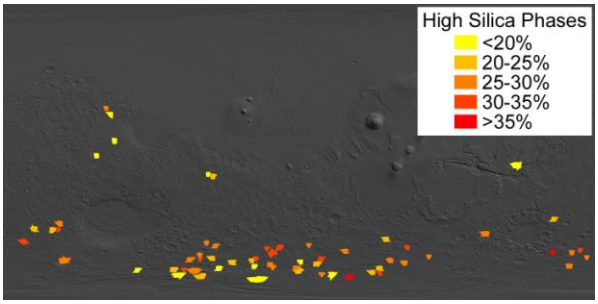

Figure 2. Global distribution of 62 dune fields, colored by High-Silica Phase group abundance. Note the high abundances at high southern latitudes.

The High-Silica Phase group abundance exceeds 25% in 36 of the 62 dune fields, despite the fact that none of the dune fields are located in Solis Planum or northern Acidalia Planitia where high-silica phases are typically this abundant [e.g., 17, 13]. Rather, the elevated abundances occur in southern mid- to high-latitudes where they have previously been identified as isolated occurrences [17,18]. However, not all of the dune fields at these latitudes have high abundances of High-Silica Phases. Most dune fields rich in High-Silica Phases are located on intercrater plains, whereas those in craters typically have lower abundances.

Dune field stability. Of those mapped, 1195 dune fields were classified with an SI confidence of 1 or 2. These are binned by latitude in **Fig. 3**. As found by [12], morphologies suggestive of aeolian stability appear south of ~60ºS. With two exceptions, most other dune fields on Mars show no signs of stabilization.

Exception #1: Some high southern latitude dune fields appear more active than their neighboring dune fields. Most of these more active-appearing dune fields are found on intercrater plains; those appearing more stabilized are more often found in craters.

Exception #2: Sixteen of 84 dune fields from 57-75ºN show minor signs of stability (SI = 2). This suggests that northern polar dunes are much more active than their southern counterparts. This correlates well with observed dune and ripple migration rates [19,20].

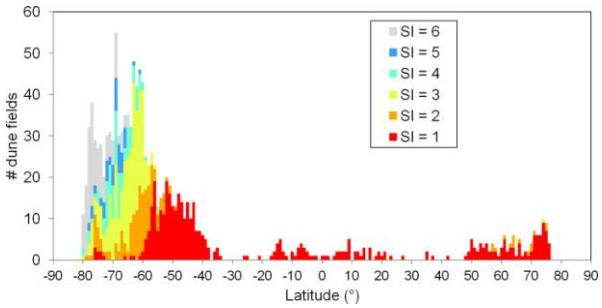

Figure 3. Latitudinally binned histogram of dune field Stability Index (SI). Note the stabilized dune fields (SI>1) at high southern latitudes and the lack of stabilized dune fields at high northern latitudes.

Discussion/Conclusions: An abundance of high-silica phases in high southern latitude dune fields correlates with milder morphological signs of stability. This association extends to the northern polar sand seas, which are both actively migrating and have a high abundance of high-silica phases. [21] found the high-silica component to be consistent with acid-leached iron-bearing glass, potentially kept free of obfuscating coatings through aeolian activity. We hypothesize that spectral signatures of acid leaching indicate aeolian activity, and thus possibly mineral maturity, in dune sands abundant in iron-bearing glass.

References: [1] Hayward et al. (2007) USGS OFR 2007-1158, doi:10.3133/20071158. [2] Hayward et al. (2010) USGS OFR 2010-1170, doi:10.3133/20101170. [3] Hayward et al. (2012) USGS OFR 2012-1259, doi:10.3133/20121259. [4] Hoover et al. (2017) *48th LPSC*, Abst. #1062. [5] Hoover et al. (2018) *49th LPSC*, Abst. #1811. [6] Christensen et al. (2009) *Fall AGU Mtg.*, Abst. #IN22A-06. [7] Edwards et al. (2011) *JGR 116*, doi:10.1029/2010JE003755. [8] Bandfield et al. (2000) *JGR 105*, doi:10.1029/1999JE001094. [9] Christensen et al. (2001) *JGR 106*, doi:10.1029/2000JE001370. [10] Rogers and Fergason (2011) *JGR 116*, doi:10.1029/2010JE003772. [11] Ahrens and Titus (2014) *8th Int'l Conf. Mars*, Abst. #1012. [12] Fenton and Hayward (2010) *Geomorphology 121*, doi:10.1016/j.geomorph.2009.11.006. [13] Rogers and Christensen (2007) *JGR 112*, doi:10.1029/2006JE002727. [14] Graham and Midgely (2000) *Earth Surf. Proc. Landf. 25*,doi: doi:10.1002/1096-9837(200012)25:13<1473::AID-ESP158>3.0.CO;2-C. [15] Tirsch et al. (2011) *JGR 116*, doi:10.1029/2009JE003562. [16] Koeppen and Hamilton (2008) *JGR 113*, doi:10.1029/2007JE002984. [17] Bandfield (2002) *JGR 107*, doi:10.1029/2001JE001510. [18] Ruff and Christensen (2007) *GRL 34*, doi:10.1029/2007GL29602. [19] Banks et al. (2018) *JGR*, in press, doi:10.1029/2018JE005747. [20] Bridges et al. (2013) *Aeolian Res. 9*, doi:10.1016/j.aeolia.2013.02.004. [21] Horgan and Bell (2012) *Geology 40*, doi:10.1130/G32755.1.